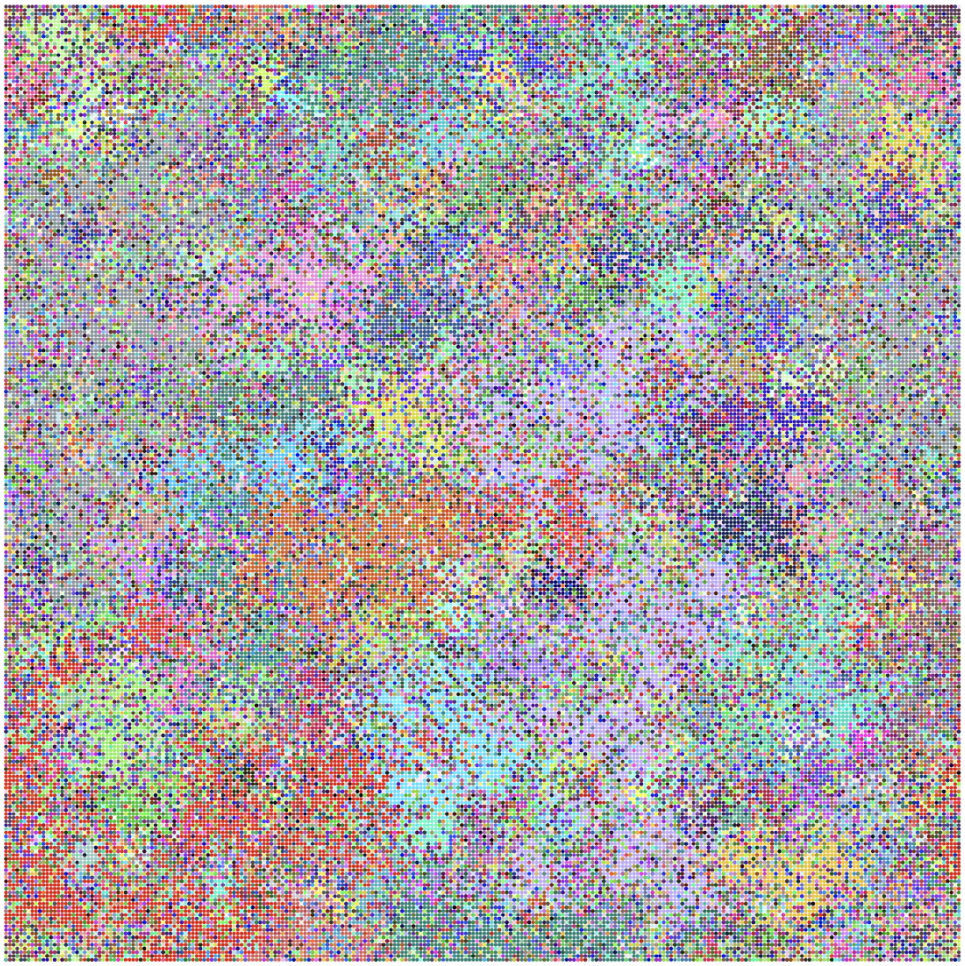
arXiv:2101.00550v1 [cond-mat.dis-nn] 3 Jan 2021

Graphical Abstract

Percolation and the pandemic

Robert M. Ziff



A system of non-planar extended-range bond percolation with $z = 68$ nearest neighbors within a radius of $\sqrt{20}$ around each site, on a square lattice at the bond threshold of $p_c = 0.019962$. Different clusters are shown as different colors, and the deep interpenetration of the clusters can be seen. This system can be considered a model of infection spreading with long but finite-0p-range connections, where different colors represent groups of infected people seeded by different people.

Highlights

Percolation and the pandemic

Robert M. Ziff

- Research highlight 1: For simple tree networks, the threshold corresponds to a critical infectivity of $R_{0,c} = (\langle z \rangle - 1)p_c = 1$
- Research highlight 2: Adding cliques to the tree increases $R_{0,c}$ when considering the outgoing bonds, thus suppressing the formation of an epidemic.
- Research highlight 3: For extended-range site or bond percolation $R_{0,c} > 1$, which implies clustering with finite-range connections also suppresses epidemics.

Percolation and the pandemic

Robert M. Ziff

Center for the Study of Complex Systems and Department of Chemical Engineering, University of Michigan, Ann Arbor, Michigan USA 48109-2800

Abstract

This paper is dedicated to the memory of Dietrich Stauffer, who was a pioneer in percolation theory and applications of it to problems of society, such as epidemiology. An epidemic is a percolation process gone out of control, that is, going beyond the critical transition threshold p_c. Here we discuss how the threshold is related to the basic infectivity of neighbors R_0, for trees (Bethe lattice), trees with triangular cliques, and in non-planar lattice percolation with extended-range connectivity. It is shown how having a smaller range of contacts increases the critical value of R_0 above the value $R_{0,c} = 1$ appropriate for a tree, an infinite-range system or a large completely connected graph.

Keywords:

1. Introduction

This paper is dedicated to the memory of Dietrich Stauffer, whose work and life had an enormous impact on me. His encouragement was unflagging, and his criticisms honest. We had many discussions about aspects of percolation including universality, thresholds, and algorithms over the years, for which I am immensely grateful.

Dietrich was the master of a quickly but clearly written paper, spontaneous, concise and to the point, something I have always tried to emulate. When explosive percolation first appeared in with the work of Achlioptas et al. [1], Dietrich suggested to me that I study it using the algorithm of Mark Newman and myself [2] on the square lattice rather than the complete

Email address: rziff@umich.edu (Robert M. Ziff)

graph as studied by the authors of [1]. I told him I was already thinking of it, and he told me it was a here and now problem and that I had to do it immediately—I had one week to get it done! In fact I finished it in four days and it ended up as a PRL [3]. For one week I acted like Dietrich.

One of the projects he repeatedly challenged me to was to find an exact expression for the site percolation threshold on the square lattice, something I had found numerically to relatively high precision ($p_c = 0.592746$) [4, 5] and sent to him in time to get it in the second edition of his book with Amnon Aharony [6], which allowed this value to be widely known. I have since worked for several years with Chris Scullard on finding exact thresholds for various lattices in two dimensions, but the square lattice with site percolation cannot be put in the self-dual form that is required to use those methods. I believe it is insoluble, but you never know—new things come along, such as the isoradial construction [7], which allowed the inhomogeneous checkerboard critical manifold to be proven [8]. In recent years, Chris and Jesper Jacobsen have found various thresholds to enormous precision using transfer matrix methods and a percolation criterion related to what had been used on self-dual systems. For the square-lattice site threshold Jacobsen found $p_c = 0.59274605079210(2)$ [9], which was independently found to 10 digits in another transfer-matrix calculation [10]. This line of work pretty much spells the end of simple Monte Carlo, at least for two dimensions where these methods apply, since, due to statistical error, straight Monte Carlo can never reach that level precision. (About 8 digits as in [11] or [12] is the maximum, since this requires at least 10^{16} random numbers to be generated.) When percolation was in its infancy, the best results were found using series, and then Monte Carlo took over. Now an analytical approach (admittedly with a lot of help from the computer) is again supreme over more brute-force Monte Carlo methods.

Several years ago there was a meeting of the German Physical Society in Bad Honnef, not far from Cologne where Dietrich lived. I visited him and he spent two days showing me around the area focusing on the political sites—things related to the war and the post-war period in a divided Germany, which interested him enormously. It was a wonderful visit. I didn't know it would be the last time I would see him.

Dietrich was a pioneer in social physics, and in applying ideas related to percolation to various social problems. Of course a problem related to percolation is epidemiology, a subject of high relevance today.

The basic problem of a spread of a disease is essentially a percolation

problem, in which individuals spread an infection to contacts which has the prospect of going out of control and infecting a large fraction of the population—exactly like a percolation transition.

The conventional approach to studying epidemiology is through the SIR (Susceptible, Infected, Recovered) model of Kermack and McKendrick [13] which dates back almost to the time of the last pandemic. This model is essentially a mean-field model in which people are put into "compartments" representing the various categories of Susceptible, Infected, Recovered, and others. When the basic reproduction number R_0, which represents the average number of people ultimately infected by one infected individual, is greater that 1, the infection can grow without bound. $R_{0,c} = 1$ is essentially the percolation threshold for this mean-field model.

When put on a lattice, the SIR model takes into account the geometry of contacts, and is in the same universality class as ordinary percolation [14, 15]). Normally one believes that a lattice model cannot be a good model for human disease spread because people travel both locally (work, shopping, entertainment, eating out) and globally (trains, air travel). During the present pandemic, however, this drawback may not be serious as people are generally less mobile (although not entirely, of course). Here, lattice-based immobile models may be more relevant. In this paper we discuss both Bethe lattice models, which are effectively infinite-dimensional, and regular lattices in two and three dimensions.

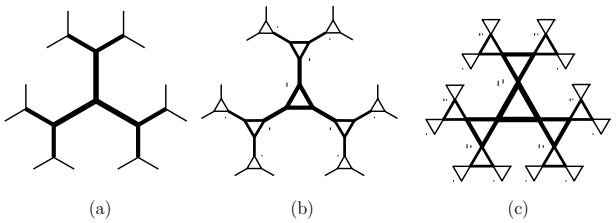


Figure 1: (a) The Bethe lattice, (b) Husimi tree with bonds, (c) Husimi tree (cactus) of triangles.

2. Bethe lattice

First we review the case where the contacts do not interfere with each other and the infection behavior is essentially as a tree. This corresponds

to the case of a Bethe lattice, or equivalently to low probability on a large fully connected graph (the Erdős-Rényi model) where the chance of loop formation is low. The Bethe lattice is discussed in detail in Stauffer and Aharony's book [6].

On a regular Bethe lattice, each node (site or vertex) is connected to z other nodes in a tree structure. An illustration of the Bethe lattice for $z = 3$ is shown in Fig. 1a. In the bond percolation problem, we assume all bonds (links) are open or occupied with probability p and closed otherwise. The bonds represent the transmission to the individual who is at the end of the bond. The percolation threshold can be found by the following simple argument: Define Q as the probability that an outgoing bond from a node does *not* connect to infinity (i.e., not be part of the percolating cluster or giant component). Q satisfies the equation

$$Q = 1 - p + pQ^{z-1} \tag{1}$$

where the term $1 - p$ represents the probability that the bond does not exist, while the second term represents the probability that the bond exists (probability p) and the $z - 1$ outgoing bonds do not connect to infinity (probability Q^{z-1}). Eq. (1) can be written

$$\begin{aligned} 1 - Q &= p(1 - Q^{z-1}) \\ &= p(1 - Q)(1 + Q + \ldots + Q^{z-2}) \end{aligned} \tag{2}$$

which yields two solutions: $Q = 1$, and the solution for $Q \leq 1$ to

$$1 + Q + Q^2 + \ldots + Q^{z-2} = \frac{1}{p} \tag{3}$$

The transition is where the two curves intersect, which is at $Q = 1$ and $p = p_c$ given by

$$p_c = \frac{1}{z - 1} \tag{4}$$

For a Bethe lattice, a spreading epidemic never encounters a previously visited site, so that all outgoing infections can potentially spread to the $z - 1$ outgoing neighbors, which are all susceptible. Thus, the average number of the outgoing neighbors that will be infected is

$$p_c(z - 1) = 1 \tag{5}$$

which we can associate with the critical value $R_{0,c}$ of $R_0 = p(z-1)$. When $R_0 > 1$, the epidemic will grow exponentially fast. Thus, for the simple Bethe lattice, the critical R_0 is equal to 1, consistent with the mean-field result that $R_0 > 1$ is the criterion for an epidemic to occur.

Of course, this shows that the larger the value of z, the probability of infecting a given neighbor p must be decreased to keep the system below the critical point. But the net number of infected neighbors at the critical point remains 1 no matter what z.

The above development can be generalized to systems with a distribution of coordination number P_z, $z = 0, 1, 2, \ldots$ for each node, where $\sum_z P_z = 1$. The distribution of neighbors from a node *connected to a randomly chosen bond* is $q_z = zP_z/\langle z\rangle_P$, where $\langle z\rangle_P = \sum_z zP_z$, because a node with z bonds attached is z times more likely to be chosen than a node with one bond, and we divide by $\langle z\rangle_P$ to normalize the distribution. The analog to Eq. (1) is now

$$\begin{aligned} Q &= 1 - p + p\sum_{z\geq 1} q_z Q^{z-1} \\ &= 1 - p + p(q_1 + q_2 Q + q_3 Q^2 + q_4 Q^3 \ldots) \end{aligned} \tag{6}$$

By the normalization of q_z we can write

$$q_1 = 1 - q_2 - q_3 \ldots \tag{7}$$

where q_1 is the probability that a node reached through a bond has one neighbor, namely the neighbor where the bond came from, so this is a terminal bond. Putting Eq. (7) in Eq. (6) yields

$$1 - Q = p[q_2(1-Q) + q_3(1-Q^2) + q_4(1-Q^3)\ldots] \tag{8}$$

which has the roots $Q = 1$ and the solution to

$$1 = p[q_2 + q_3(1+Q) + q_4(1+Q+Q^2) + \ldots] \tag{9}$$

At $Q = 1$, this equation yields the threshold [16]

$$p_c = \frac{1}{\langle z\rangle_q - 1} \tag{10}$$

where

$$\langle z\rangle_q = \sum_{z\geq 1} zq_z = \frac{1}{\langle z\rangle_P}\sum_{z\geq 1} z^2 P_z = \frac{\langle z^2\rangle_P}{\langle z\rangle_P} \tag{11}$$

The quantity $\langle z\rangle_q$ represents the average coordination of nodes connected to a randomly chosen bond. Again, this threshold corresponds to the point where the outgoing bonds have an average occupancy of one:

$$R_{0,c} = p_c(\langle z\rangle_q - 1) = 1. \tag{12}$$

Note that Eq. (10) also can be found by writing $Q = 1+\epsilon$ and expanding Eq. (6) about $\epsilon = 0$, since that equation has a double root at $Q = 1$ when you are at the threshold p_c. The relation between q_z and P_z is discussed more in Ref. [17].

As a specific example, consider the case where $P_3 = 0.9$ and $P_{10} = 0.1$—that is, 90% the nodes have coordination number 3 and therefore 2 outgoing neighbors, and 10% the nodes have coordination number 10 and therefore 9 outgoing neighbors. Then $\langle z\rangle_P = (0.9)(3) + (0.1)(10) = 3.7$, $\langle z^2\rangle_P = 18.1$, $\langle z\rangle_q = 4.892$ and $p_c = 0.2569$ according to Eq. (10). If all nodes had coordination number $z = 3$, then p_c would be equal to $1/2$. Thus, having just 10% of the nodes with $z = 10$ reduces the threshold almost in half and greatly increases the risk of an epidemic occurring for a fixed p.

Note that in the example above $q_3 = 27/37$ and $q_{10} = 10/37$. Thus, if you pick a site randomly, its average number of neighbors is $\langle z\rangle_P = 3P_3+10P_{10} = 3.7$, but if you look at a neighboring site of that randomly selected site (or the site connected to a randomly selected bond), the average coordination of that site is $\langle z\rangle_q = 3q_3+10q_{10} = 4.892$—that is, your neighbor is likely to have more neighbors than you have. This is an example of the phenomenon that your friends are likely to have more friends that you have, and is a general feature of networks where the distribution of neighbors is inhomogeneous.

As another example, we consider the case of a Bethe lattice where the distribution of z around a given site follows a Poisson distribution with mean λ:

$$P_z = \frac{\lambda^z}{z!}e^{-\lambda} \tag{13}$$

which satisfies $\sum_{z=0}^{\infty} P_z = 1$. Then $\langle z\rangle_P = \lambda$, $\langle z^2\rangle_P = \lambda+\lambda^2$, and $\langle z\rangle_q = \lambda+1$, and it follows from Eq. (10) that $p_c = 1/\lambda$. Note that the average coordination number of a randomly chosen node $\langle z\rangle_P$ and the average coordination number of a node connected to a randomly chosen bond $\langle z\rangle_q$ differ by exactly 1 here; so here it turns out that $p_c = 1/\langle z\rangle_P$, which is not generally the case.

Another way to interpret the above result is that if one creates a network with a Poisson distribution with $\lambda > 1$, and each bond is occupied with

probability p, then the distribution of occupied bonds would also be a Poisson distribution, but with mean $p\lambda$ and threshold $p_c = 1/\lambda$. If one makes a network (or Bethe lattice) with a Poisson distribution at $\lambda = 1$, then the system is right at the percolation point when all the bonds are occupied ($p_c = 1$). If one has a Poisson distribution network with $\lambda < 1$, the system will never percolate.

The complete graph, or Erdős-Rényi model, is one in which all N nodes of a system are connected together by $N(N-1)/2$ links, so every node has exactly $N-1$ neighbors. If we consider occupying a small fraction of those bonds with $p(N-1)$, the probability of forming loops will be small, and the coordination around each point will be a binomial distribution with mean $p(N-1)$. In the limit of large N this distribution becomes the Poisson distribution with mean $\lambda = pN$. and the threshold will be at $p_c = 1/N$. The ER graph is at the critical point if the mean number of outgoing bonds is equal to 1, just as in the Bethe lattice. For all examples of a Bethe lattice, the threshold corresponds to $R_{0,c} = p_c(\langle z \rangle_q - 1) = 1$.

3. Percolation on the Bethe lattice with internal triangles.

Here we consider is a variation of the Husimi lattice or a cactus with triangles connected to bonds in a tree structure, as shown in Fig. 1b. We will consider only a three-branched system here; the mathematics can be generalized to a larger clique in the center and more branches. Such systems have been used in the study of the spread of diseases (i.e., [18]. First we consider a general system in which the triangle in the center is a 3-bond (or 2-simplex) characterized by $\mathcal{P}_0$ = probability that none of the three vertices are connected together, $\mathcal{P}_2$ = the probability that one given pair of vertices are connected together (all three possible pairs having equal probability), and $\mathcal{P}_3$ = the probability that all three vertices are connected together, such that

$$\mathcal{P}_0 + 3\mathcal{P}_2 + \mathcal{P}_3 = 1 \tag{14}$$

Then, for Q we have

$$Q = 1 - p + p(\mathcal{P}_0 + \mathcal{P}_2 + 2\mathcal{P}_2 Q + \mathcal{P}_3 Q^2) \tag{15}$$

where $\mathcal{P}_0 + \mathcal{P}_2$ represents the events in which the outer vertices will not connect to the incoming vertex of the triangle, $2\mathcal{P}_2$ represents the two ways

there will be one connection, and $\mathcal{P}_3$ represents the event in which both outgoing vertices connect to the incoming one.

Writing $\mathcal{P}_0 = 1 - 3\mathcal{P}_2 - \mathcal{P}_3$ and substituting into Eq. (15), we find

$$1 - Q = p[2\mathcal{P}_2(1 - Q) + \mathcal{P}_3(1 - Q^2)] \tag{16}$$

which once again has a root at $Q = 1$, and a second one at $1/p = 2\mathcal{P}_2 + (1 + Q)\mathcal{P}_3$, and the threshold is determined by the crossing point where $Q = 1$, yielding the criticality condition

$$1 = 2p(\mathcal{P}_2 + \mathcal{P}_3) \tag{17}$$

where $\mathcal{P}_2$ and $\mathcal{P}_3$ can also depend upon internal bond probabilities.

When $p = 1$, we have simply that the threshold is determined by $\mathcal{P}_2 + \mathcal{P}_3 = 1/2$, or, using Eq. (14), the condition

$$\mathcal{P}_3 = \mathcal{P}_0/2 + 1/4 \tag{18}$$

This can be compared with the condition $\mathcal{P}_0 = \mathcal{P}_3$ that applies to a regular lattice hypergraph of 3-bonds that fall on a self-dual arrangement [19]. The system here is a tree version of the generalized kagome lattice, which has been studied in Refs. [20] and [21], where it was found that $\mathcal{P}_3(\mathcal{P}_0) \approx 0.52732 + 0.83886(P_0 - 0.096523) + \ldots$ which is an expansion about an exactly soluble point, where the behavior to first-order is also linear.

Now we consider that the 3-bond is indeed a simple triangle of three bonds, each occupied with probability r. Then $\mathcal{P}_0 = (1-r)^3$, $\mathcal{P}_2 = r(1-r)^2$ and $\mathcal{P}_3 = r^3 + 3r^2(1 - r)$ and Eq. (17) yields the critical curve on the p-r plane as

$$1 = 2p(r + r^2 - r^3) \tag{19}$$

If $p = r$, that is all bonds on the network have the same probability, then Eq. (19) predicts $p_c = 0.637278$. This is a tree version of the $(3, 12^2)$ which on a regular lattice has a threshold of $p_c = [1 - 2\sin(\pi/18)]^{1/2} = 0.807901$ [22], as expected a higher value than for the tree. For the two outgoing bonds leaving the triangle, the net $R_{0,c}$ is $2p_c = 1.615802$, well above the value of 1. This is a consequence of the clique reducing transmission through it.

When $p = 1$, we have the pure triangular husimi lattice with no bonds linking them together as shown in Fig. 1c, and the threshold is determined by Eq. (19), with solution $r_c = 0.403032$. This is a tree version of the kagome lattice, where the bond threshold is 0.524405 [23, 24], again a higher value.

If we look at a given infected individual, and consider three out of four of the bonds at a vertex being outgoing bonds, then $R_0 = 3r_c = 1.20910$. This shows that by making the network composed of closed loops (while overall still a tree), the threshold will correspond to a higher R_0, and the closed loops attenuate the probability of an epidemic.

Another model to consider is that either all three of the individuals in the triangular clique become infected (probability $\mathcal{P}_3 = r$), or none of them become infected ($\mathcal{P}_0 = 1 - r$), with $\mathcal{P}_2 = 0$. In other words, we are replacing the triangle by a site and making this the site-bond percolation problem on the Bethe lattice. Here we have from Eq. (17) simply $pr = 1/2$ for the critical curve. When $r = 1$ we have the usual $z = 3$ Bethe lattice bond threshold $p_c = 1/2$ and $R_{0_c} = 2p_c = 1$. Now, however, by lowering r below 1, we can increase R_0 based on the outgoing bonds, $R_{0,c} = 2p_c = 1/r$. The minimum value of r is $1/2$, at which point p_c becomes 1 and the system becomes pure site percolation on the Bethe lattice, with $R_0 = 2$. Having a probability less than 1 of infecting the other people in your group (i.e., decreasing r) helps in slowing the epidemic.

While unrelated to the epidemic problem, we note that Eq. (17) is valid for correlated bonds or three-site interactions. (Of course, the site-bond problem above is also an example of correlated bonds within the triangle.) For example, consider a system where $\mathcal{P}_0 = 0$, where every triangle has at least one bond in it. The nomralization condition $3\mathcal{P}_2 + \mathcal{P}_3 = 1$ and the criticality condition $\mathcal{P}_2 + \mathcal{P}_3 = 1/2$ (Eq. (17) with $p = 1$) implies $\mathcal{P}_2 = \mathcal{P}_3 = 1/4$, or it is equally likely that a triangle is in each of the one-bond states or in the fully connected state. The fully connected triangles triangles ($\mathcal{P}_3$) act as branches, and the other triangles act as single bonds, or dead-ends if the bond is one opposite side of a triangle from a given path. This is reminiscent to a model on the regular triangular lattice where each "up" triangle has exactly one bond, which is also at the critical point [19].

4. Percolation on lattices with extended-range non-planar connections

In ordinary bond percolation, the edges or bonds are independently occupied with probability p, and connected nodes (sites) make clusters or graph components. When carried out on a regular lattice, this leads to the commonly studied models of percolation.

For a spread of an epidemic, a lattice percolation model has the virtue that it can take spatial effects such as blocking into account. For most situations, a simple two-dimensional lattice would not be appropriate, because of longer-range transmission through travel etc. However, in the present Covid-19 pandemic, travel (both on large and small scales) has been drastically curtailed, so lattice percolation may possibly be a useful model.

For a spreading epidemic, we have the same situation as in the Bethe lattice where the disease enters through one bond. The $(z-1)$ remaining bonds are available for spreading. Assuming there is no other infection in this region of the lattice, the average number of bonds that carry the infection to new sites will be $p(z-1)$. Thus, if we again associate R_0 with $p(z-1)$, the critical value of R_0 will be

$$R_{0,c} = p_c(z-1) \tag{20}$$

For example, for bond percolation on the square lattice, where $z = 4$ and $p_c = 1/2$, this implies that $R_{0,c} = 3/2$. We see that this is significantly larger than the critical value ($R_{0,c} = 1$) of the Bethe lattice, because many of the growth paths of the epidemic on a lattice are blocked by encounters with previously infected sites during the growth process.

However, it is more relevant to have a longer range of contact included in the model beyond the nearest neighbor. This can be incorporated into percolation by adding long but finite-range bonds to the neighborhood of the individuals, who sit at the sites of the lattice. One can think of the longer-range (or extended-range) bonds as representing a limited amount of mobility for individuals.

The study of extended-range non-planar percolation goes back to the equivalent-neighbor model of Domb and Dalton [25], where site percolation was studied with several extended neighborhoods on a variety of lattices. Other site percolation models were studied by Gouker and Family [26], Galam and Malarz [27], d'Iribarne et al. [28], and many others [29, 30, 31, 32, 33, 34]. Here we are more interested in bond percolation, where an occupied bond represents the spread of an infection to a susceptible individual within the allowed neighborhood. Bond percolation on lattices with extended neighborhoods has been studied more recently [35, 36, 34, 37, 38]. Another related model is long-range percolation which has an infinite range and a power-law bond probability distribution [39, 40, 41].

In table 1 we show results for p_c (from different sources and calculations here) and $R_{0,c} = (z-1)p_c$ for models of bond percolation with a neighborhood

Table 1: Bond percolation thresholds for square lattice with circular neighborhoods up to radius r, showing the coordination number z (number of nearest neighbors to a site) and the maximum nearest neighbor (NN) considered. Values come from the references cited in superscripts, except $z = 24$, 44, 56, 68 and 80, which we determined here using a single-cluster growth procedure[34] and a method based upon a universal fluctuation ratio[42].

r^2	z	NN	p_c	$(z-1)p_c$
1	4	1	0.5	1.5
2	8	2	0.2503685[35]	1.7526
4	12	3	0.1522203[35]	1.6744
5	20	4	0.0841509[35]	1.5989
8	24	5	0.067185	1.5453
9	28	6	0.0558493[35]	1.5079
10	36	7	0.04169608[35]	1.4594
13	44	8	0.032971	1.4178
16	48	9	0.02974268[35]	1.3979
17	56	10	0.02489	1.3690
18	60	11	0.0230119[35]	1.3577
20	68	12	0.019962	1.3373
25	80	13	0.016517	1.3048
49	148	23	0.008342595[35]	1.2264
72	224	32	0.0053050415(33)[35]	1.1830
225	708	86	0.001557644(4)[36]	1.1013
389	1224	141	0.000880188(90)[35]	1.0765
489	1652	185	0.000645458(4)[36]	1.0657
961	3000	317	0.000349601(3)[36]	1.0485
1280	4016	413	0.0002594722(11)[35]	1.0418

in the region of a disk of radius r, namely with long range bonds that extend to all sites (x, y) about a given site (x_0, y_0) such that $(x-x_0)^2+(y-y_0)^2 \leq r^2$. Note that for $r > 1$ there are crossing bonds such that paths of different clusters can cross each other without intersecting, so these models represent non-planar systems.

For the calculations here, we used the single-cluster growth method [43, 34] with a maximum cutoff of $s = 16384$ or 65536 occupied sites, and used the fact that near p_c, the probability a site is connected to a cluster of size greater than or equal to s is expected to behave as

$$P_{\geq s} \sim A s^{\tau-2}[1 + B(p - p_c)s^{\sigma} + Cs^{-\Omega}] \tag{21}$$

where $\tau - 2 = 5/91$, $\sigma = 36/91$, and $\Omega = 72/91$ in 2D. This is valid for p very close to p_c and s large. At p_c, a plot of $s^{\tau-2}P_{\geq s}$ vs. $s^{-\Omega}$ yields a straight line, as shown in Fig. 2 for $z = 68$. Note that we are finding consistency with the usual 2D value of τ here; for very large z, one might expect Bethe-lattice behavior $\tau = 5/2$ for smaller s, but we did not see that here.

We also verified this result by using the union-find simulation method [44], monitoring the largest cluster s_{max} and its square, and finding their average values and the ratio $Q = \langle s_{\max}^2 \rangle / \langle s_{\max} \rangle^2$. This quantity has the universal value of 1.04149 in 2D, for systems with a square periodic boundary [42]. In a shorter amount of time than in the single-cluster simulations and in a single run, taking a lattice of size 1024×1024 and using 10^6 samples, we were able to verify the value $p_c = 0.0199616(2)$ as the point where $Q = 1.04149$ for $L = 2048$ (270,000 samples). This method was also used for finding p_c for $z = 24$, 44, 56, and 80 also. These simulation results support that non-planar percolation is in the normal universality class of ordinary percolation, including the ordinary critical exponents and universal fluctuation ratio Q.

In Fig. 3 we plot $R_{0,c} = (z-1)p_c$ as a function of $\ln z$, For large z, the asymptotic behavior $R_{0,c} = 1$ is obtained, but for smaller z there is a marked increase, with a peak of $R_{0,c} = 1.7526$ at $z = 8$ but then drops off fairly slowly with z. This shows that by restricting possible contacts to a finite range, the critical infection rate will be substantially larger than 1, so that it is less likely for an epidemic to spread for a given R_0.

Note that the large-z behavior of p_c for bond percolation is expected to behave as [45]

$$(z-1)p_c(z) \sim 1 + cz^{-1/2} \tag{22}$$

(The authors of Ref. [45] consider zp_c rather than $(z-1)p_c$, but to this order in z the behavior is the same.) In Fig. 4 we plot $(z-1)p_c$ as a function of $z^{-1/2}$, and it clearly can be seen that the large-z behavior satisfies this expected form, with $c = 2.756$. (A related plot is given in Ref. [38], Fig. 9, which also verifies the same asymptotic behavior.) Note that the neighborhoods within a distance of radius r are not exactly the same shape, because of the lattice effect, so one might expect some deviations from a smooth behavior. Nevertheless, the adherence to linear behavior on this plot is quite good. In Ref. [45], in Corollary 1.3, the authors reference results of a computer simulation that implies $c = 1.2\sqrt{\pi} = 2.13$, which is a bit below the value here and the difference is likely a result of a lower level of statistics in that work.

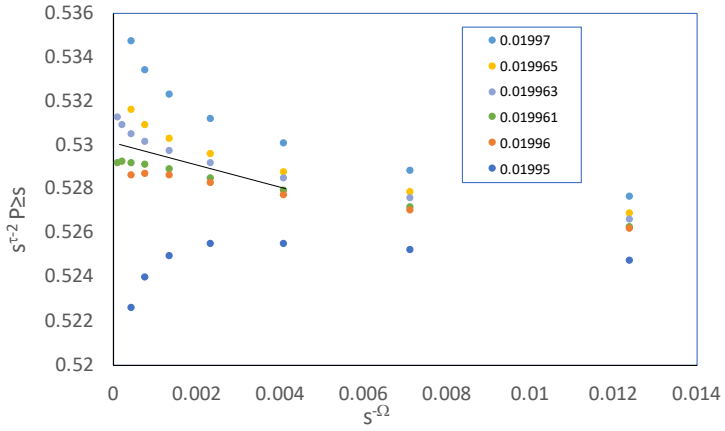


Figure 2: Determination of the bond percolation threshold for $r = \sqrt{20}$ or $z = 68$ using the single-cluster growth algorithm. A plot of $s^{\tau-2}P_{\geq s}$ vs. $s^{-\Omega}$ for different p. The two central curves suggest a threshold of $p = 0.019962(1)$. Here the cutoff was taken as $s_{\max} = 16384$ except the two central curves with $s_{\max} = 65536$. Up to 10^8 runs were made for each value of p, including the two systems with the larger cutoff. The line goes through the average of the points for $p_c = 0.019961$ and 0.019963 and shows the expected behavior at the critical point.

In Fig. 5 we make a similar plot for 3D extended-range bond percolation, using data from Ref. [34] for smaller z and from more recent work [46] for larger z up to $z = 250$. We find the data are consistent with a correction of order $z^{-2/3}$ as predicted in Ref. [45], providing a better fit than assuming a correction of $z^{-1/2}$ as in 2D (Eq. (22)) and was used in our previous paper [34]. Further work for even larger z is needed to demonstrate the correction behavior clearly.

5. Epidemics and extended-range site percolation

In extended-range site percolation with circular neighborhoods, all occupied sites that are within a circle of radius r of a given occupied site will be connected to that site through long bonds of length greater than one lattice spacing. In terms of epidemiology, site percolation corresponds to saying that an infected individual will infect all susceptible neighbors within a radius r, and the rest of the sites within that radius will never become susceptible or infected.

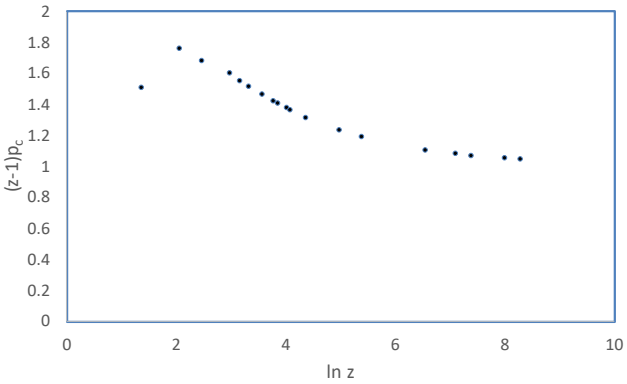


Figure 3: Plot of $R_{0,c} = (z-1)p_c$ vs. $\ln z$ using the data of table 1 (2D percolation)

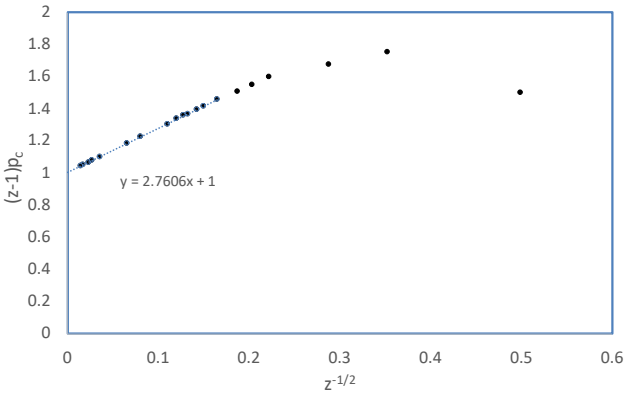


Figure 4: Plot of $R_{0,c} = (z-1)p_c$ vs. $z^{-1/2}$ using the data of table 1 (2D percolation). The linear fit for the data for $z \geq 36$ yields a slope of 2.76.

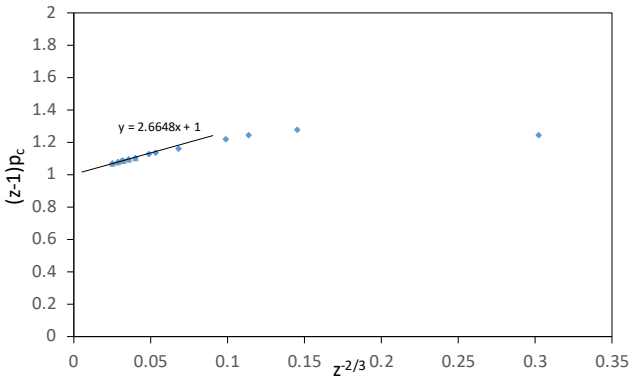


Figure 5: Plot of $R_{0,c} = (z-1)p_c$ vs. $z^{-2/3}$ for the 3D extended-range bond percolation data of Refs. [34] and [46]. The peak in $R_0 = (z-1)p_c$ is lower here than the peak in 2D systems. The line with slope 2.665 fits the six points of data from $z = 146$ to 250, and supports the prediction that the corrections go as $z^{-1/3}$

Extended-range site percolation differs from extended-range bond percolation in that the former is effectively planar while the latter can be non-planar — that is, paths of clusters can cross each other in extended-range bond percolation, but cannot in extended-range site percolation. In site percolation, one assumes that infected individual will infect all the people within the range of interaction and there are no additional susceptible individuals within that range, which is not the case for bond percolation.

For large r, the extended-range site percolation becomes equivalent to the continuum percolation of overlapping disks of radius $r/2$, because two disks of that radius will just touch when their centers are a distance r apart, and the centers of the disks is where we consider the infected individuals to reside. In continuum percolation of disks, the critical coverage fraction of disks of radius $r/2$ (including overlapping areas) is defined as

$$\eta_c = \pi(r/2)^2 \frac{N}{V} \tag{23}$$

where N is the number of disks in a region of area V and $\eta_c = 1.12809$ [38, 47, 48]. Then $p = N/V$ is effectively the occupation of sites when the continuum percolation is superimposed on a lattice. The number of possible neighbors on the lattice is $z = \pi r^2$, and putting this all together yields [34]

$$zp_c = 4\eta_c = 4.5123 \tag{24}$$

so once again the threshold is inversely proportional to z, but with a different coefficient than in bond percolation, where the coefficient is 1 as in Eq. (22). From the epidemic perspective, this means that you can infect up to 4.5 people in your circle of influence and not have the epidemic spread. This is because those and subsequent people will have a smaller area of susceptible people to infect, because of the overlap of the disks of influence. While in bond percolation, each individual has to infect just a little over one other individual to trigger an epidemic, but eventually more people within the circle of radius r might eventually become infected by other bonds. It is an interesting question for future study to ask how many individuals within that radius r of the first site eventually become infected through the bond percolation process, by means for direct paths and indirect paths.

Thus, the site percolation result says that if people keep fewer than $R_{0,c} = 4.5123$ other people within their circle, the epidemic will not spread (assuming that the people are spread randomly over a two-dimensional surface).

6. Discussion

For a mean field or Bethe-tree behavior, one would expect that the critical value of the infection number R_0 is 1. Putting groups of people in a clique or otherwise making the tree have loops increases the critical R_0 above 1. Furthermore, putting the individuals on a plane such as a square lattice with a limited range of infection also has the effect of increasing the critical $R_{0,c}$ above the value of 1, considering both site and bond percolation models. Clearly, from a public health perspective, clustering people and restricting the range that people can interact can inhibit the spread of a disease, and we can see that percolation theory provides a quantitative explanation of this.

It should be emphasized that in spite of the observation that for many systems $R_{0,c} > 1$, the mean-field SIR model with $R_{0,c} = 1$ remains very useful as a simple set of differential equations for understanding how various factors affect the spread of a disease and for easily finding the time dependence.

Here we assume the individuals are stationary but interact over possibly long but finite range bonds. The universality class of these models is still that of ordinary percolation. It is possible that the class may change if movement of the individual is also added to the models, as was studied in [49].

Here we considered just a square lattice. It may also be interesting to look at a triangular lattice or even a random one such as the Voronoi lattice or the Delaunay triangulation, although one would expect the behavior to be

qualitatively similar. Higher dimensional lattices might be useful to model more complex interactions. A direct study of lattice versions of the SIR model with extended-range interactions should also be interesting. Another question to look at are the dynamics on various lattice structures such as small-world and other fractal networks. This might explain the power-law growth behavior seen in some regimes of Covid epidemics [41, 50, 51].

7. Acknowledgments

The author thanks Ivan Kryven for comments, and Chris Scullard for comments and for preparing Fig. 1.

References

[1] D. Achlioptas, R. M. D'Souza, and J. Spencer, Science **323**, 1453 (2009).

[2] M. E. J. Newman and R. M. Ziff, Phys. Rev. Lett. **85**, 4104 (2000).

[3] R. M. Ziff, Phys. Rev. Lett. **103**, 045701 (2009).

[4] R. M. Ziff and B. Sapoval, J. Phys. A: Math. Gen **19**, L1169 (1986).

[5] R. M. Ziff and G. Stell, unpublished. (1990).

[6] D. Stauffer and A. Aharony, *Introduction to Percolation Theory, 2nd ed.* (CRC press, 1994).

[7] G. R. Grimmett and I. Manolescu, Probability Theory and Related Fields **159**, 273 (2014).

[8] R. M. Ziff, C. R. Scullard, J. C. Wierman, and M. R. A. Sedlock, J. Phys. A: Math. Th. **45**, 494005 (2012).

[9] J. L. Jacobsen, J. Phys. A: Math. Th. **48**, 454003 (2015).

[10] Y. Yang, S. Zhou, and Y. Li, Entertainment Computing **4**, 105 (2013).

[11] X. Feng, Y. Deng, and H. W. J. Blöte, Phys. Rev. E **78**, 031136 (2008).

[12] S. Mertens and C. Moore, Phys. Rev. E **98**, 022120 (2018).

[13] W. O. Kermack and A. G. McKendrick, Proc. Roy. Soc. London. A **115**, 700 (1927).

[14] P. Grassberger, Math. Biosciences **63**, 157 (1983).

[15] T. Tomé and R. M. Ziff, Phys. Rev. E **82**, 051921 (2010).

[16] M. Molloy and B. Reed, Random Structures & Algorithms **6**, 161 (1995).

[17] I. Kryven, R. M. Ziff, and G. Bianconi, Phys. Rev. E **100**, 022306 (2019).

[18] I. Iacopini, G. Petri, A. Barrat, and V. Latora, Nature Comm. **10**, 2485 (2019).

[19] R. M. Ziff and C. R. Scullard, J. Phys. A: Math. Gen. **39**, 15083 (2006).

[20] R. M. Ziff and H. Gu, Phys. Rev. E **79**, 020102 (2009).

[21] C. R. Scullard, J. L. Jacobsen, and R. M. Ziff, arXiv: 2009.01913 [cond-mat.stat-mech] (2020).

[22] P. N. Suding and R. M. Ziff, Phys. Rev. E **60**, 275 (1999).

[23] R. M. Ziff and P. N. Suding, J. Phys. A: Math. Gen. **30**, 5351 (1997).

[24] C. R. Scullard and J. L. Jacobsen, Phys. Rev. Research **2**, 012050 (2020).

[25] C. Domb and N. W. Dalton, Proc. Phys. Soc. **89**, 859 (1966).

[26] M. Gouker and F. Family, Phys. Rev. B **28**, 1449 (1983).

[27] S. Galam and A. Mauger, Phys. Rev. E **53**, 2177 (1996).

[28] C. d'Iribarne, M. Rasigni, and G. Rasigni, Phys. Lett. A **263**, 65 (1999).

[29] T. R. Gawron and M. Cieplak, Acta Phys. Pol. A **80**, 461 (1991).

[30] Ł. Kurzawski and K. Malarz, Rep. Math. Phys. **70**, 163 (2012).

[31] M. Majewski and K. Malarz, Acta Phys. Pol. B **38**, 2191 (2007).

[32] K. Malarz, Phys. Rev. E **91**, 043301 (2015).

[33] K. Malarz, arXiv: 2006.15621 [cond-mat.stat-mech] (2020).

[34] Z. Xun and R. M. Ziff, Phys. Rev. E **102**, 012102 (2020).

[35] Y. Ouyang, Y. Deng, and H. W. J. Blöte, Phys. Rev. E **98**, 062101 (2018).

[36] Y. Deng, Y. Ouyang, and H. W. J. Blöte, J. Phys.: Conf. Ser. **1163**, 012001 (2019).

[37] Z. Xun, D. Hao, and R. M. Ziff, arXiv: 2010.02895 [cond-mat.stat-mech] (2020).

[38] W. Xu, J. Wang, H. Hu, and Y. Deng, arXiv: 2010.02887 [cond-mat.stat-mech] (2020).

[39] L. M. Sander, C. P. Warren, and I. M. Sokolov, Physica A **325**, 1 (2003).

[40] P. Grassberger, Physica A **153**, 289 (2013).

[41] U. Tirnakli and T. C. (2020), Front. Phys. **8**, 613168 (2020).

[42] H. Hu, H. W. J. Blöte, and Y. Deng, J. Phys. A: Math. Th. **45**, 494006 (2012).

[43] C. D. Lorenz and R. M. Ziff, Phys. Rev. E **57**, 230 (1998).

[44] M. E. J. Newman and R. M. Ziff, Phys. Rev. E **64**, 016706 (2001).

[45] S. Frei and E. Perkins, Electron. J. Probab. **21**, 56 (2016).

[46] Z. Xun and R. M. Ziff, to be published (2021).

[47] Y. Y. Tarasevich and A. V. Eserkepov, Phys. Rev. E **101**, 022108 (2020).

[48] S. Mertens and C. Moore, Phys. Rev. E **86**, 061109 (2012).

[49] P. M. C. de Oliveira, Physica A **561**, 125287 (2021).

[50] R. M. Ziff and A. L. Ziff, MedRxiv preprint , doi:10.1101/2020.02.16.2002382 (2020).

[51] G. Bianconi and P. L. Krapivsky, Phys. Rev. E **102**, 032305 (2020).